Analysis of Multispectral Land Surface Reflectance Time-Series for Detecting and Classifying Land Cover Change

*Srija Chakraborty, USRA/ GSFC, *ASU*

Profs. Antonia Papandreou-Suppappola, Philip Christensen, ASU

November 12, 2020

Arizona State University

schakr34@asu.edu, srija.chakraborty@nasa.gov

Change Detection from Frequently Acquired Observations

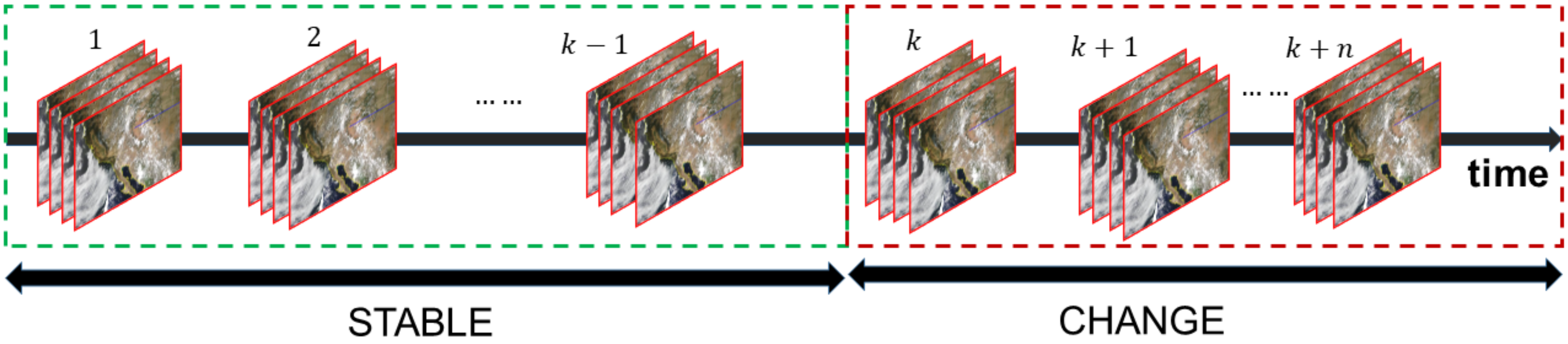

- State of the land surface can change with time
- Observations of land cover images are available only sequentially
- Adapt to spatial variability
- Direct time-series, model (harmonic) based (Lunetta et. al. 2006, Lhermitte et. al. 2008, Kleynhans et. al. 2011, Anees et. al. 2015, Chakraborty et. al. 2018)
- Cannot distinguish between types of changes; application specific bands/band ratio monitored
- Generalized change detection approach
- Examine the separability of change events by exploiting multispectral behavior over time

Features from Satellite Image Time-Series

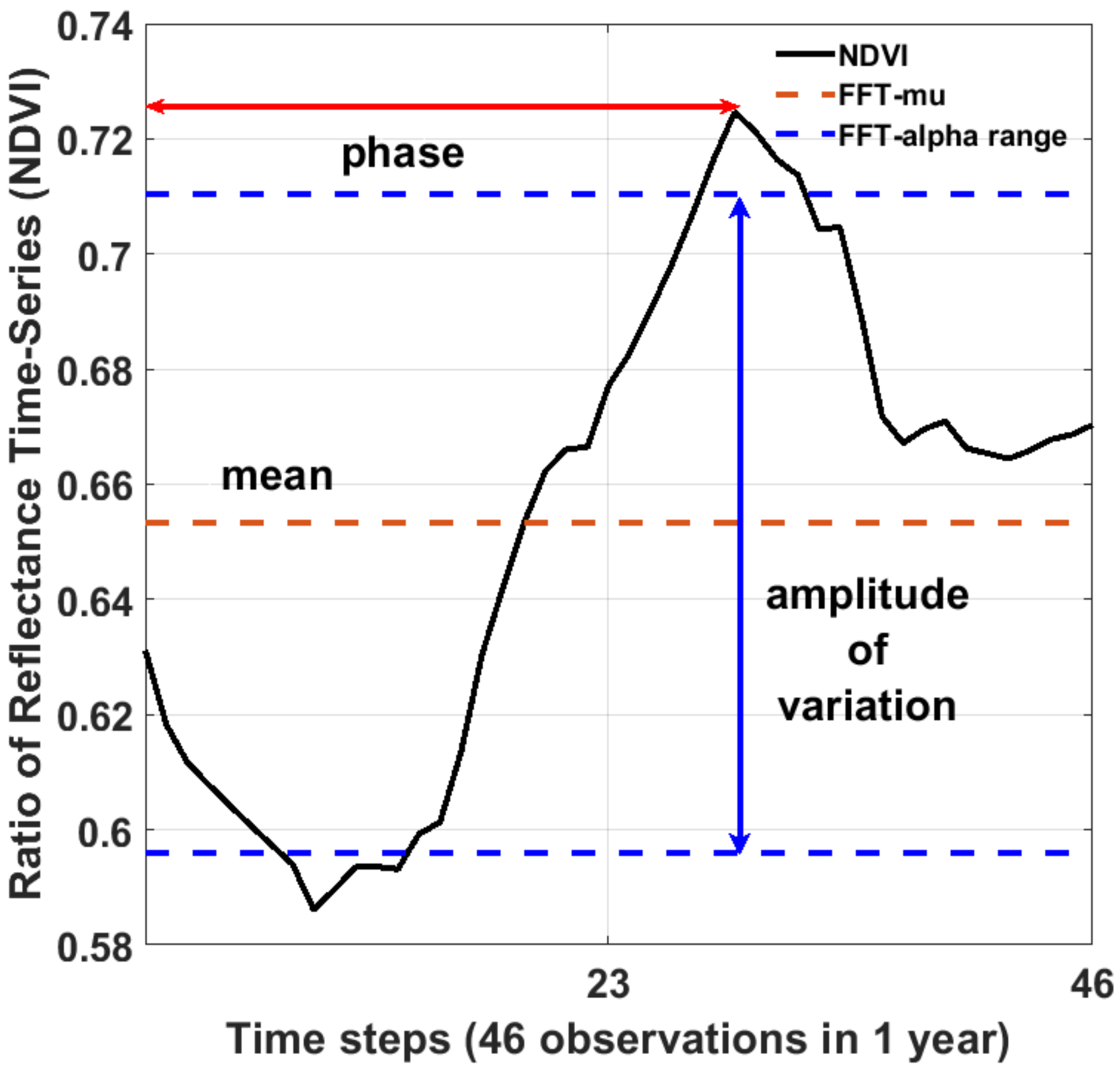

- Extracting seasonal parameters using Fourier transform
  - mean, μ
  - amplitude, α
  - phase, φ
- Characteristic features of the region/ land cover class
- Class separability
- Time variation (k) captured from sequential estimation of $\boldsymbol{x}_k = [\mu_k, \alpha_k, \varphi_k]$
- Extend estimation to all bands b, $\boldsymbol{x}_{b,k}$

Sequential Model Parameter Estimation

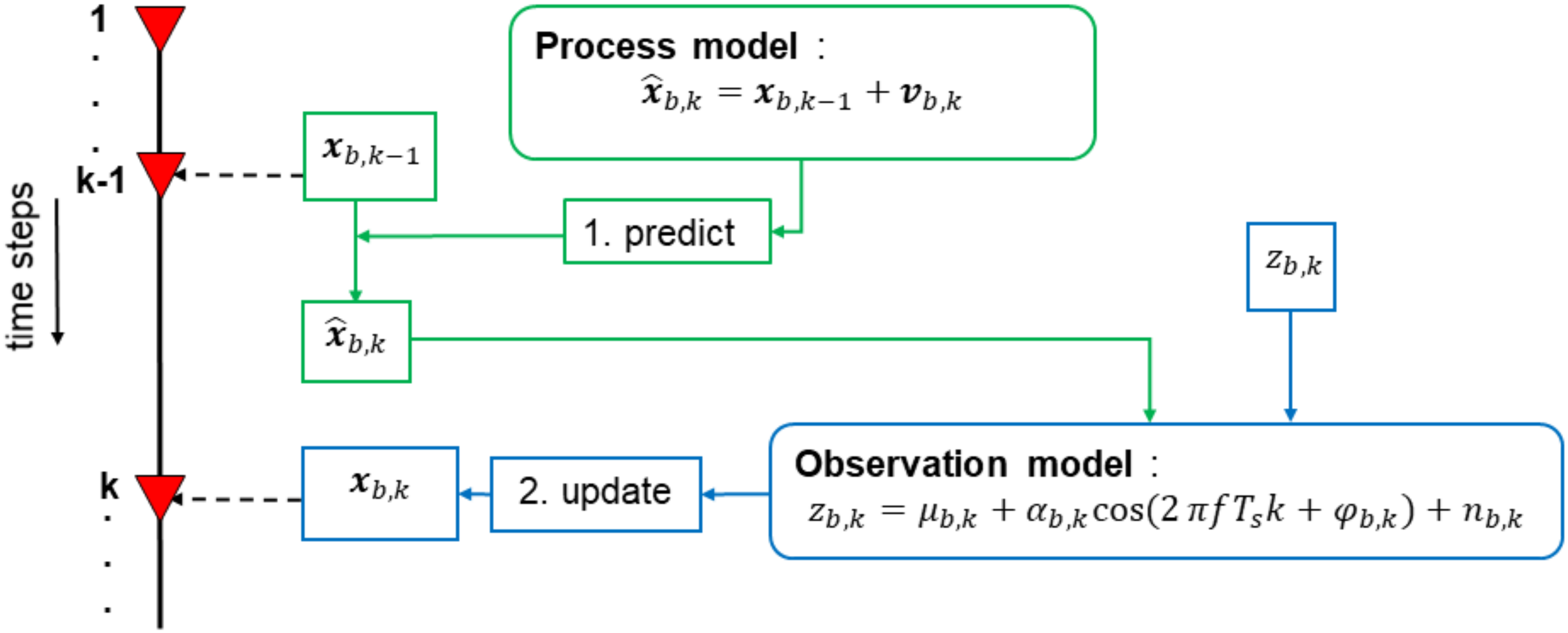

Sequential estimation of state vector $\boldsymbol{x}_{k,b} = [\mu_{k,b}, \alpha_{k,b}, \varphi_{k,b}]$ with Particle Filtering

Learning Expected Spectral Reflectance – Absence of Change

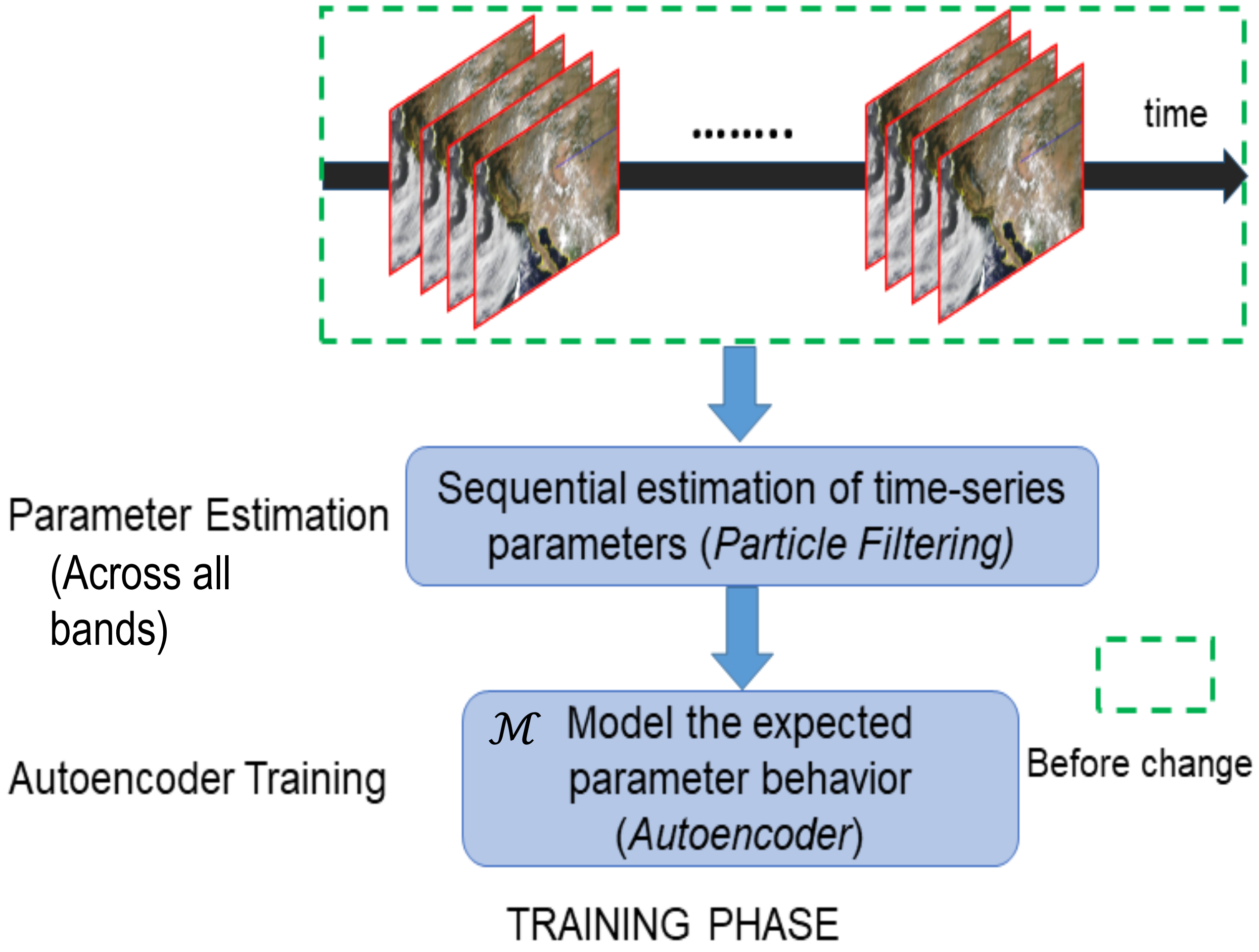

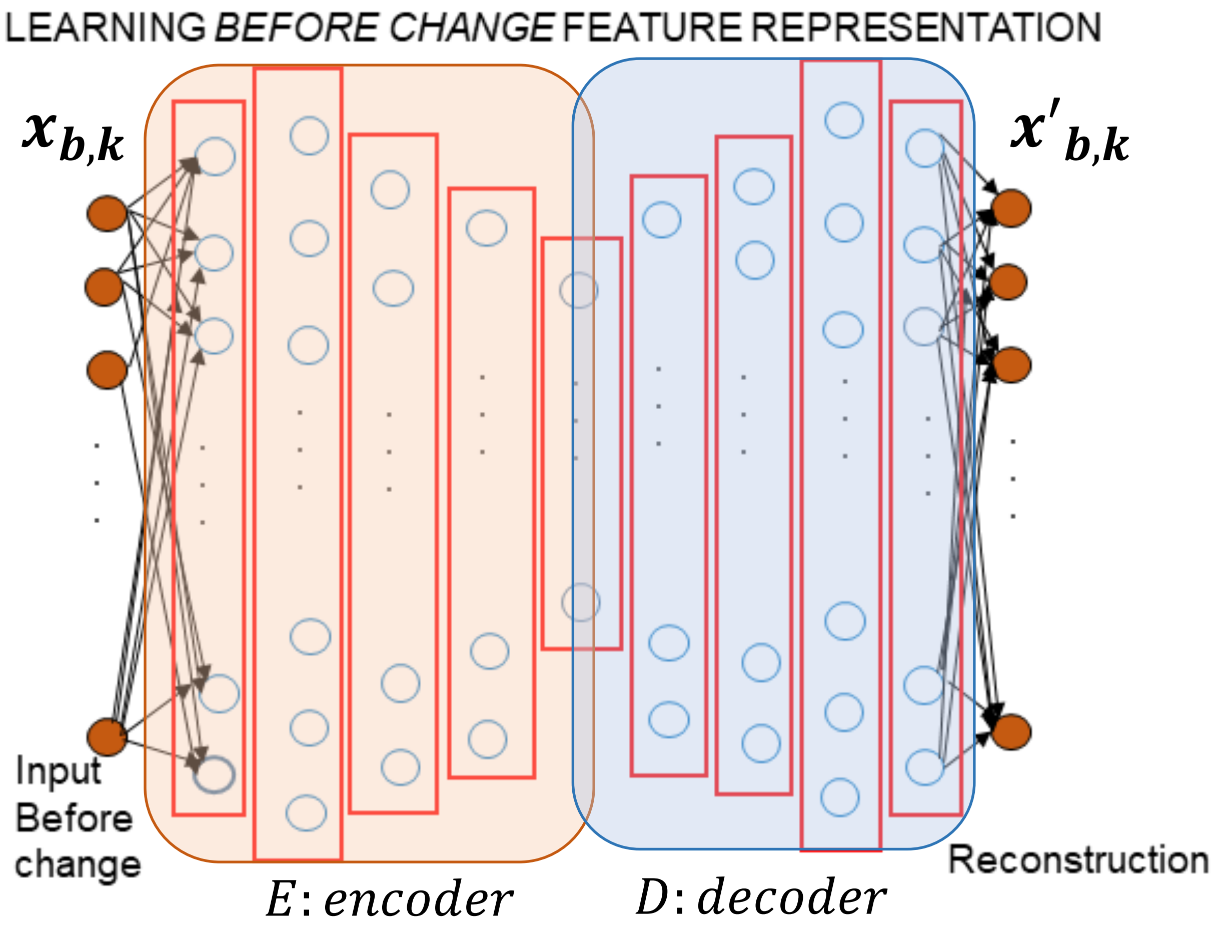

$\boldsymbol{x}_{b,k}$: μ, α ($\mathcal{M}$-all)

$\boldsymbol{x}_{b,k}$: μ ($\mathcal{M}$-mean)

$\boldsymbol{x}_{b,k}$: z ($\mathcal{M}$-obs)

$\boldsymbol{x}'_{b,k} = D(E(\boldsymbol{x}_{b,k}))$, for all k in training phase

$\mathcal{M}$: Expected Stable Phase Multispectral Trend

Multispectral Analysis at Change Point

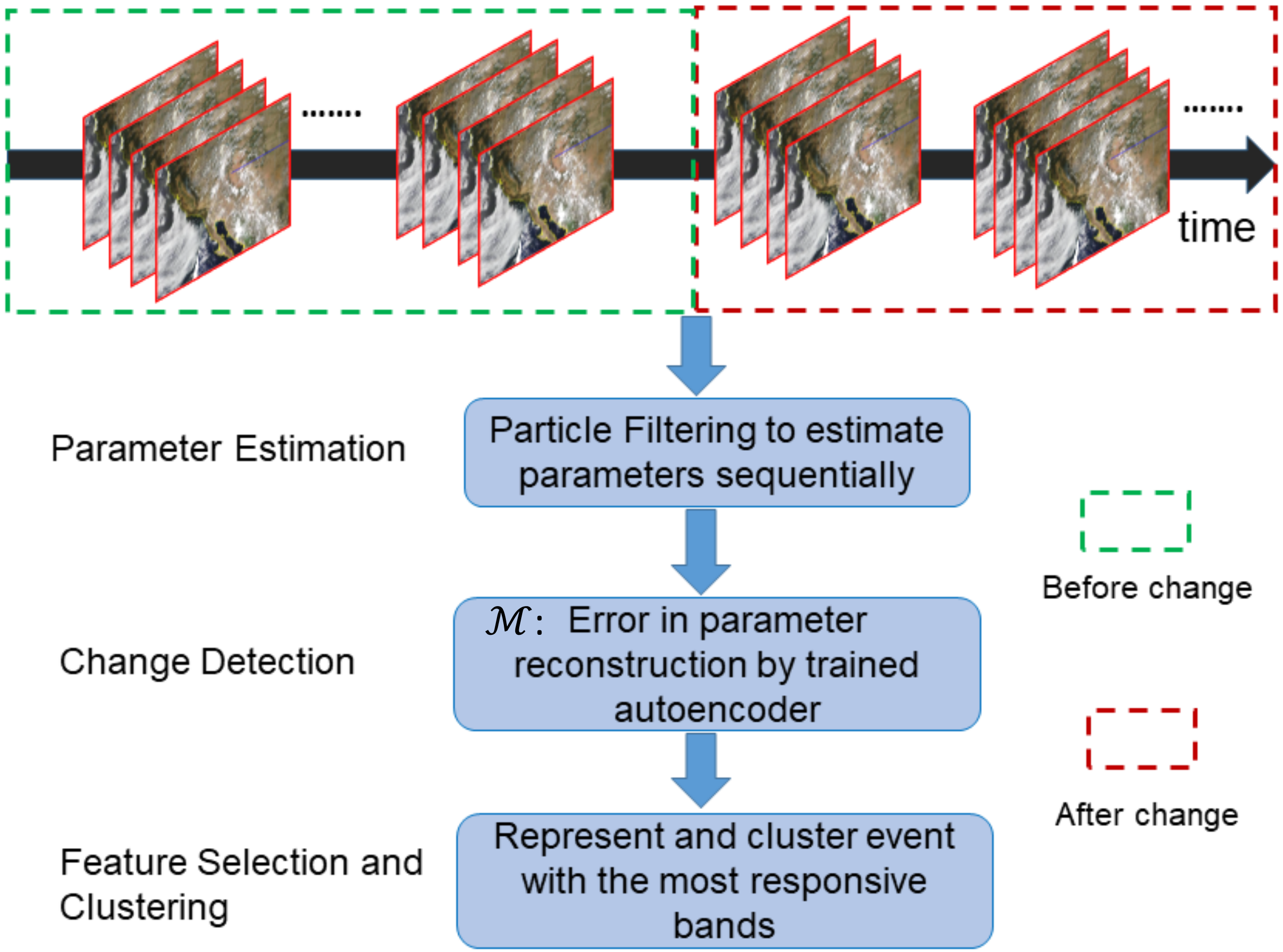

TESTING AND CLASSIFICATION

Dataset: Change Events

- Multispectral MODIS Land surface time-series
  - (MCD43A4)
- 16 day composite generated every 8 days
- 500 m
- Quality Assurance Data(MCD43A2)
- Pixel time-series of bands, band ratios
- 7 bands: 459 nm – 2155 nm

Dataset (Region)	Event, (No. of Pixels Selected), Time-Series Length	Pre-Change Land Cover Class* and event
CR1 (v5h8)	Wallow Fire, (95), 10 years	Forest Fire in Evergreen Forest
CR2 (v5h8)	Horseshoe 2 Fire, (60), 10 years	Forest Fire in Evergreen Forest
CR3 (v6h10)	Flood (Hurricane), (45), 7 years	Flood in Coastal Wetland
CR4 (v4h19)	Flood (Sava River), (35), 7 years	Flooding in Cultivated Area, Croatia
CR5 (v4h19)	Flood (Sava River), (30), 7 years	Flooding in Cultivated Area, Bosnia Herzegovina
CR6 (v6h10)	Coastal Land Gain, (30), 16 years	Coastal Land Gain (Atchafalaya Bay)
CR7 (v5h8)	Drought, (35), 13 years	Drought in Evergreen Forest

*NLCD 2016 : https://www.mrlc.gov/viewer/

*https://www.eea.europa.eu/data-and-maps/figures/global-landcover-2000-europe-geographic-view

Anomaly Score from Multispectral Analysis

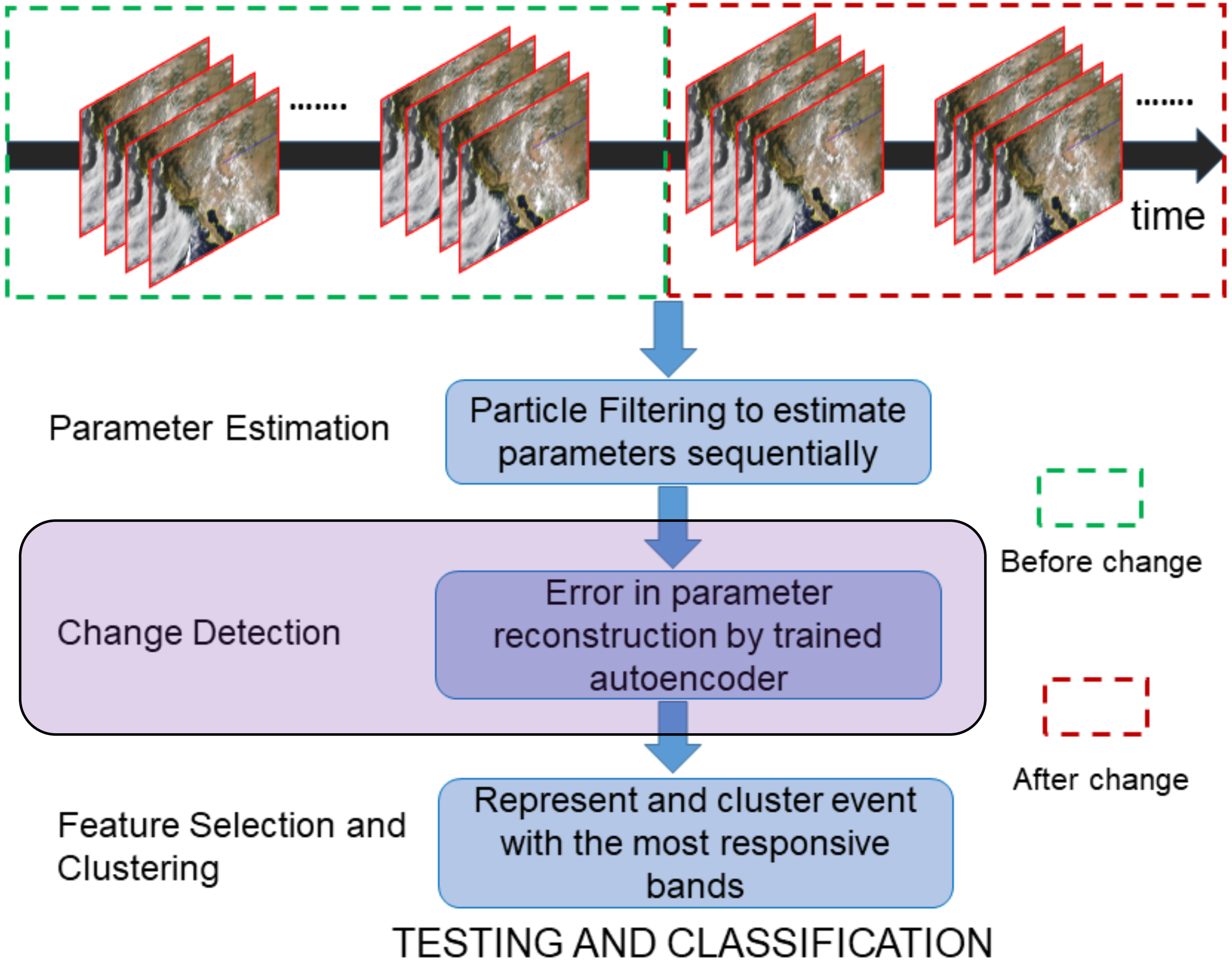

Anomaly Score: $A_k = \sum_{b=1}^{B} |\boldsymbol{x'}_{b,k} - \boldsymbol{x}_{b,k}|$

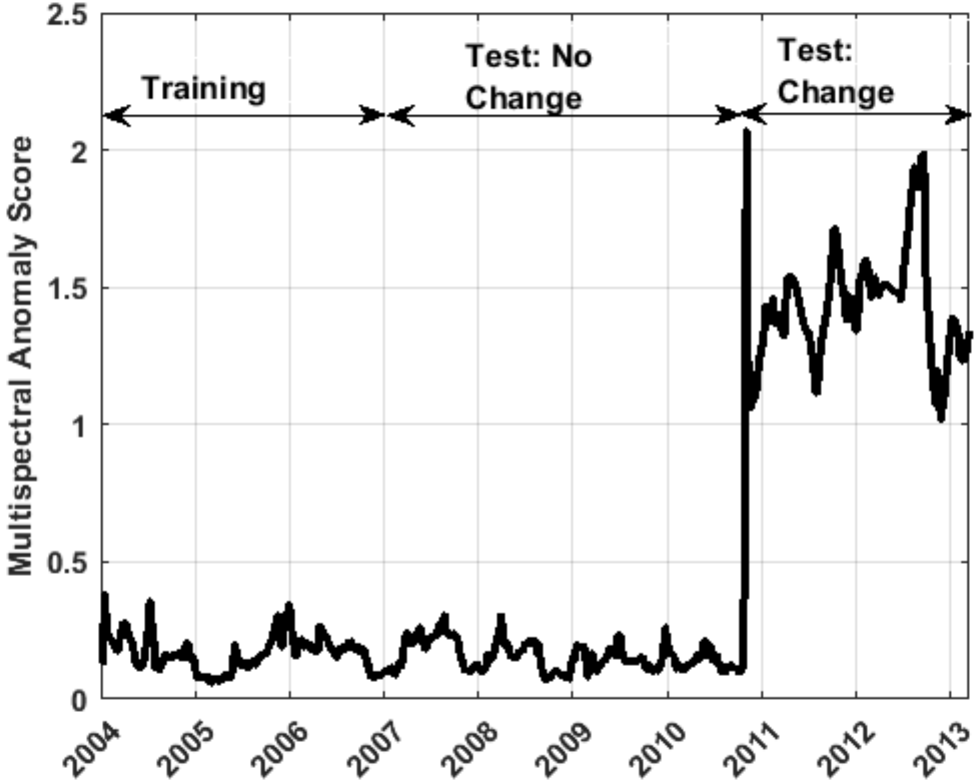

Change Detection from Multispectral Deviation

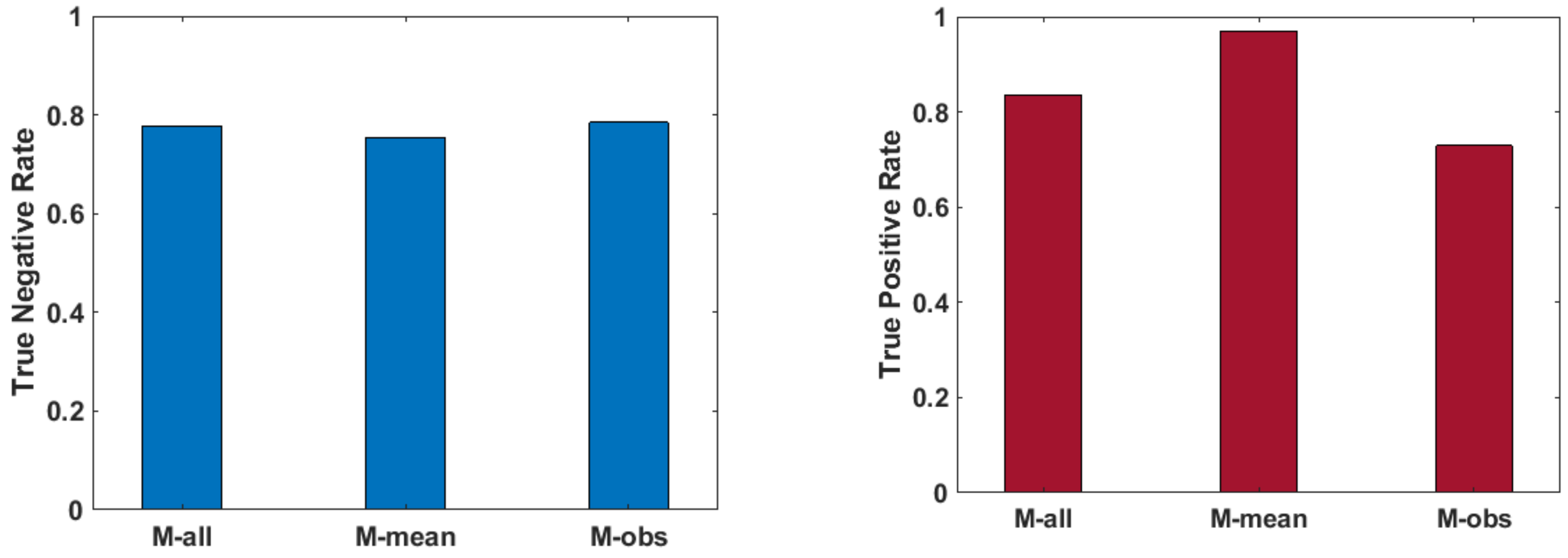

$\boldsymbol{x}_{\boldsymbol{b},\boldsymbol{k}}$: μ, α ($\mathcal{M}$-all) $\boldsymbol{x}_{\boldsymbol{b},\boldsymbol{k}}$: μ ($\mathcal{M}$-mean) $\boldsymbol{x}_{\boldsymbol{b},\boldsymbol{k}}$: z ($\mathcal{M}$-obs)

Anomalous/change points: positive class; Non-change points: negative class; TN: True negative, TP: True Positive, FN: False Negative, FP: False Positive

$$TNR = \frac{TN}{TN + FP} \qquad TPR = \frac{TP}{TP + FN}$$

PF estimates performs better (missed detections are more costly, false alarms within an acceptable rate)

S. Chakraborty, S. Das, P. R. Christensen, and A. Papandreou-Suppappola, "On the Separability and Explanations of Land Cover Change Events from Multispectral MODIS Time-Series "

Change Event Separability from Spectral Deviation

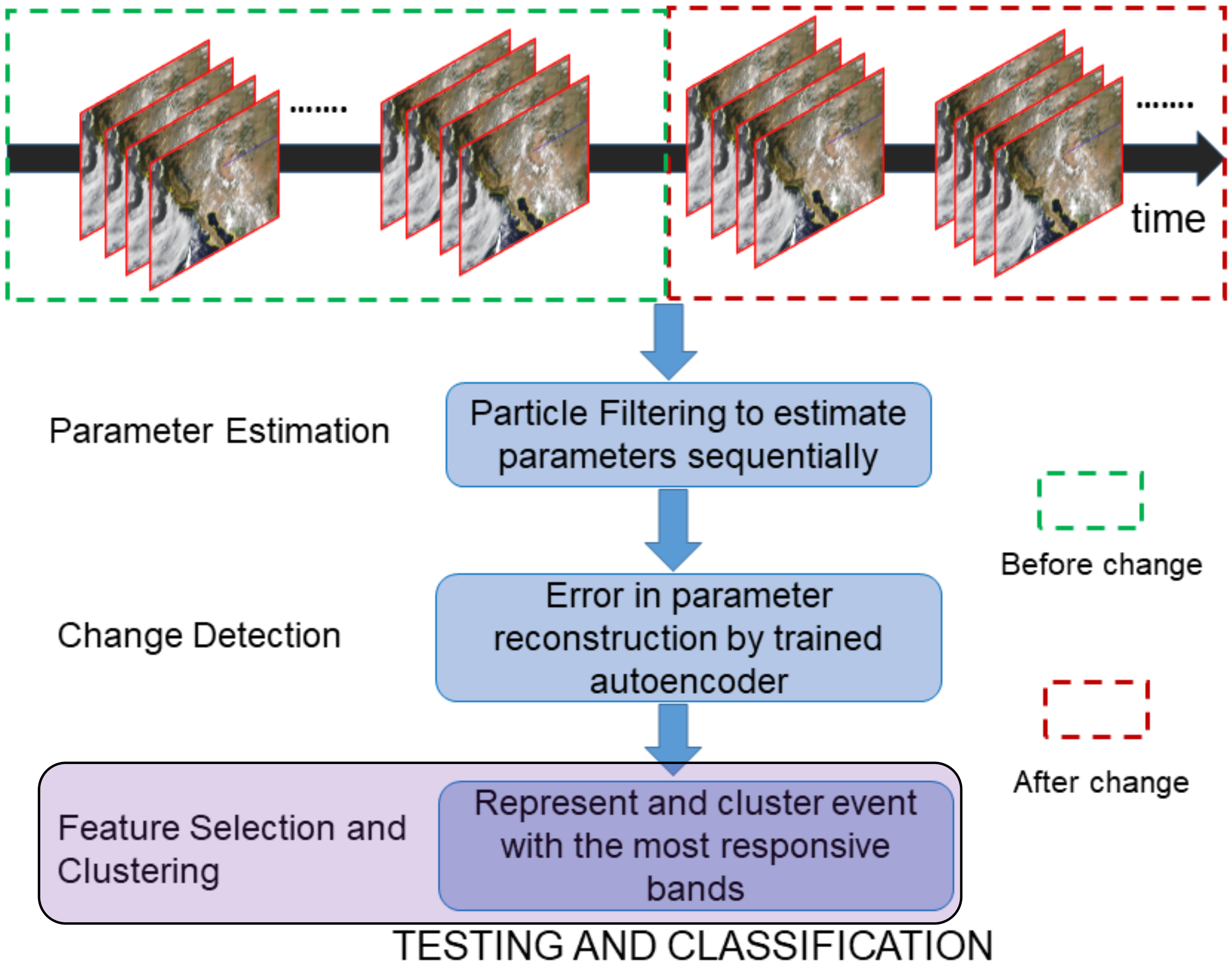

Sequentially Estimated reflectance ($\boldsymbol{x}_{b,k}$)
Reconstructed reflectance: ($\boldsymbol{x}'_{b,k}$)

Reconstructed reflectance ($\boldsymbol{x}'_{b,k}$) at k greater than estimated reflectance ($\boldsymbol{x}_{b,k}$)?

$$\left(\boldsymbol{x}'_{b,k} - \boldsymbol{x}_{b,k}\right) > 0$$

Time-series (at k in band b) decreases due to change

Reconstructed reflectance ($\boldsymbol{x}'_{b,k}$) at k lesser than PF estimated reflectance ($\boldsymbol{x}_{b,k}$)?

$$\left(\boldsymbol{x}'_{b,k} - \boldsymbol{x}_{b,k}\right) < 0$$

Time-series (at k in band b) increases due to change

Change Event Separability from Spectral Deviation

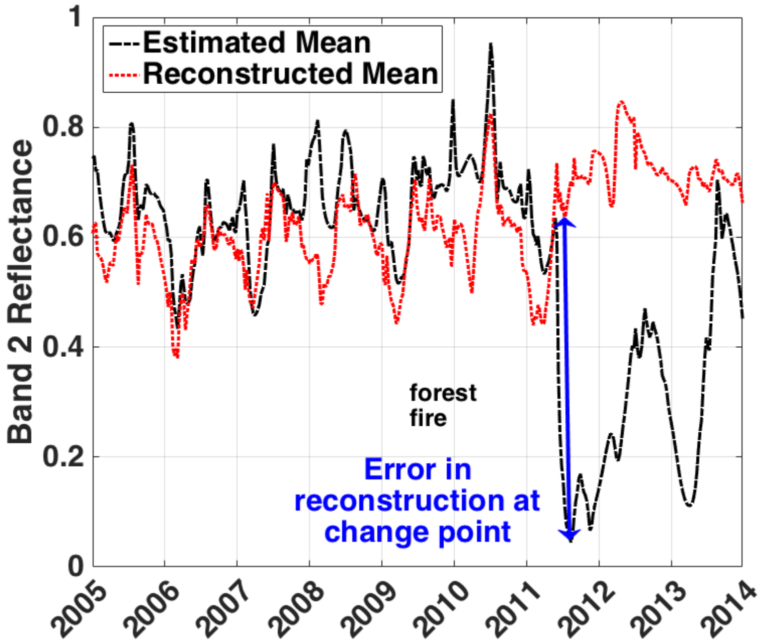

NIR Reflectance Decreases

841-876 nm

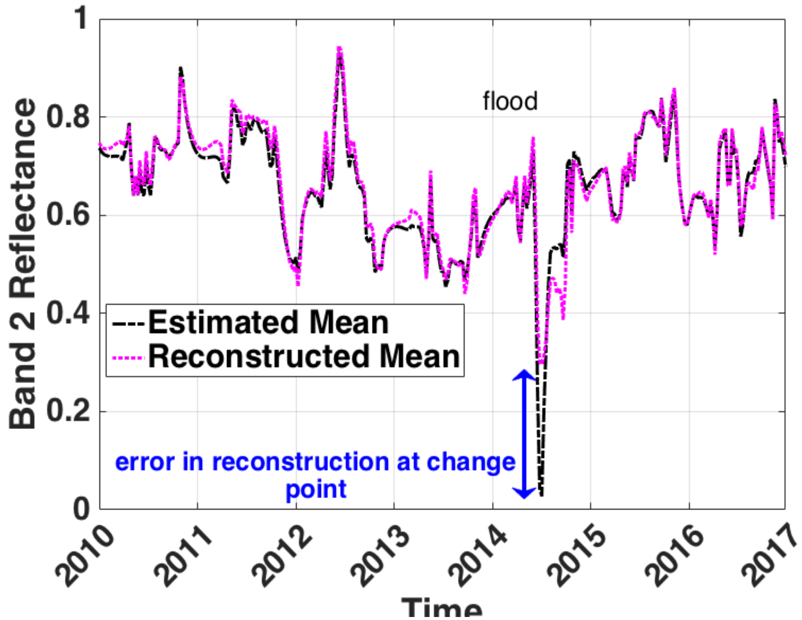

NIR Reflectance Decreases

841-876 nm

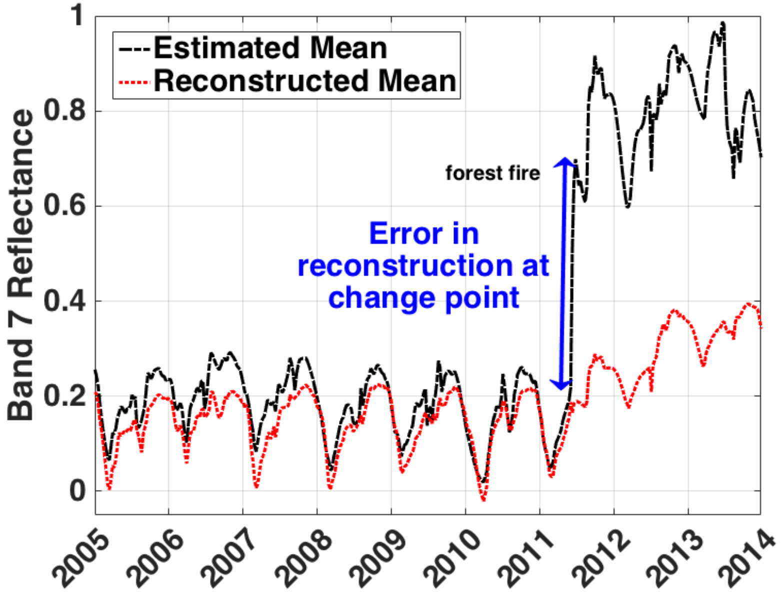

SWIR Reflectance Increases

2105-2155 nm

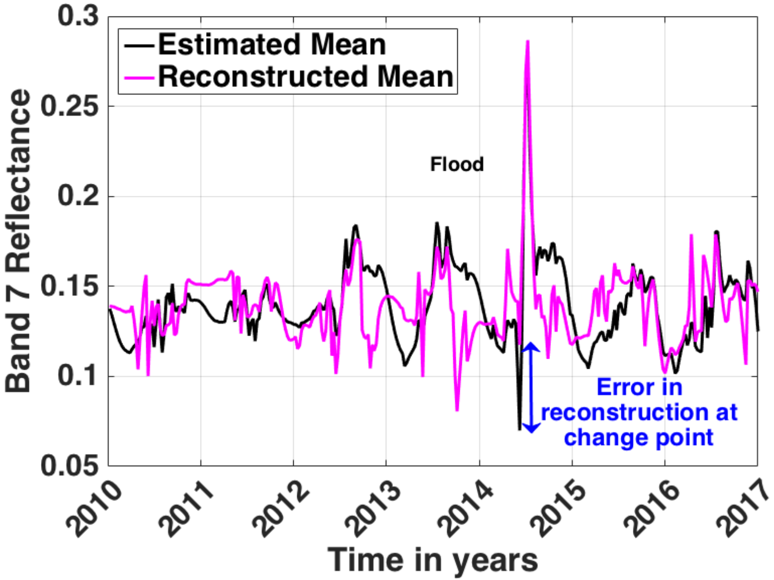

SWIR Reflectance Decreases

2105-2155 nm

Interpreting Change Signatures

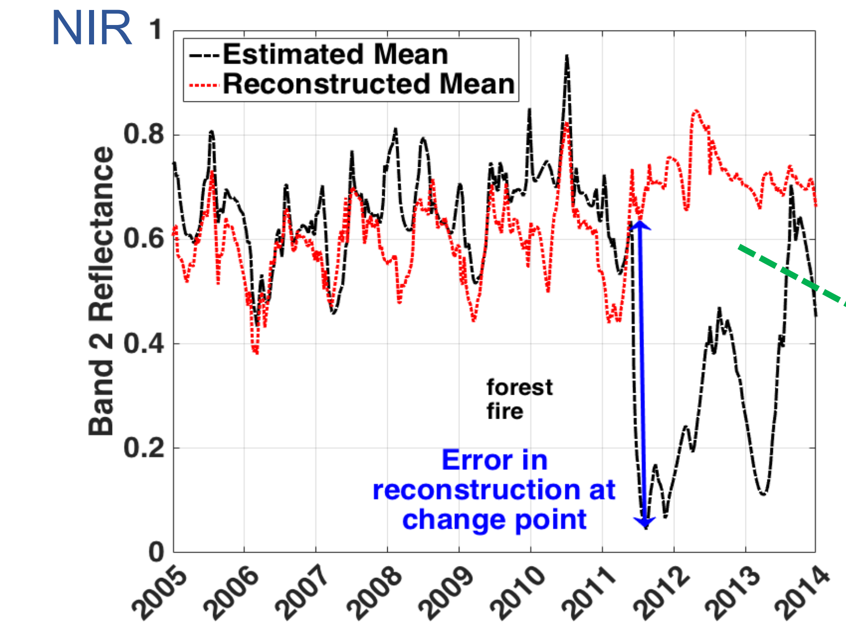

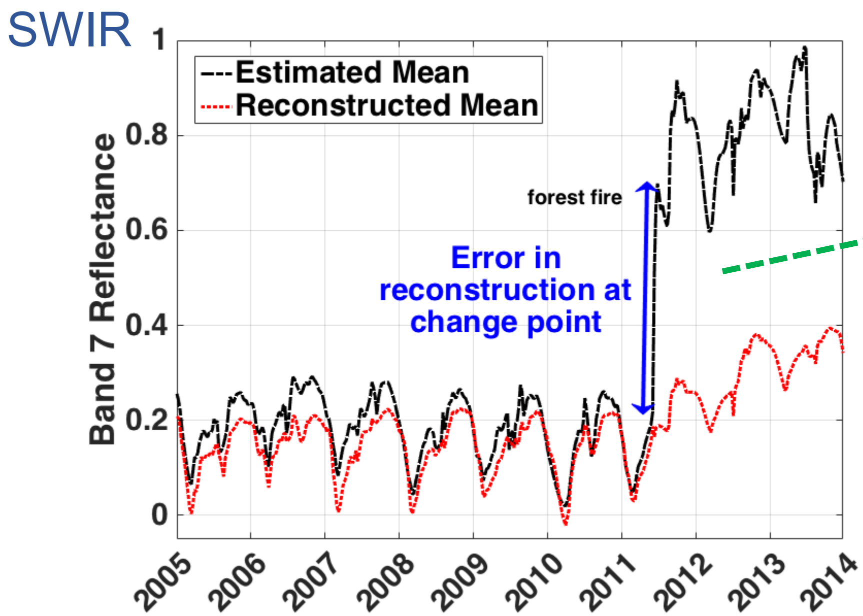

r_b=estimate (PF) ($\boldsymbol{x}_{b,k}$) – reconstruction (model) ($\boldsymbol{x'}_{b,k}$)

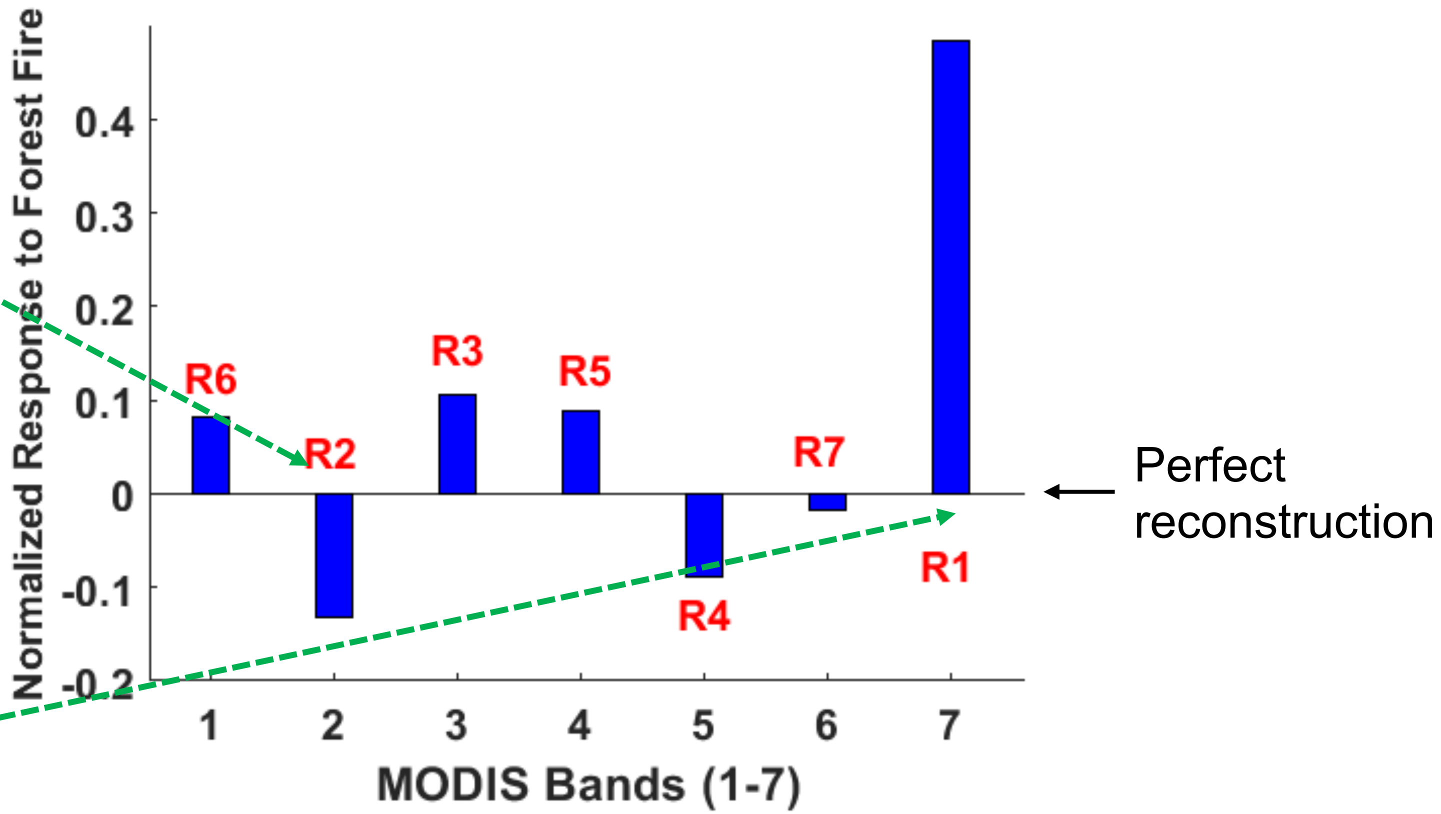

R1-R7: rank/ contribution of each band towards the reconstruction error

Different bands contribute differently (r_b) to the reconstruction error of change events

Change Signature Representation

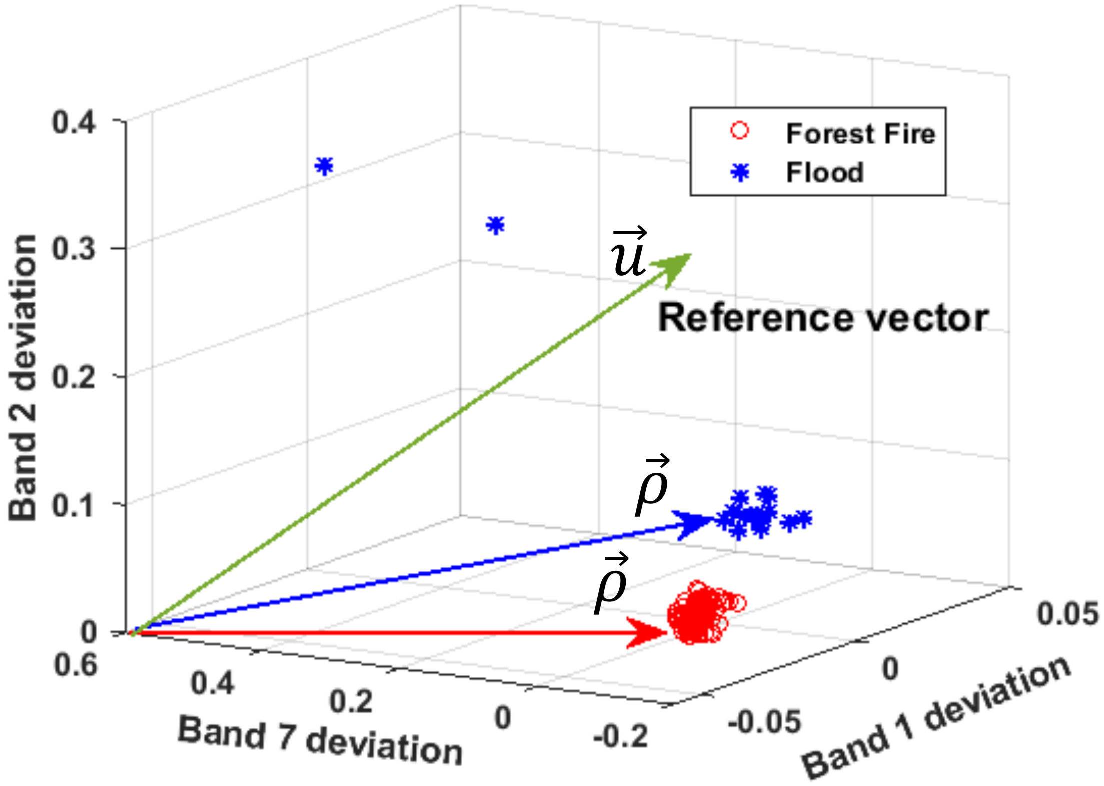

$$\vec{\rho} = [r_{b1}, r_{b2}, \ldots, r_{b7}],$$
$$\text{response at change point and post} - \text{change stages}$$

Vector representation of deviation due to change events (subset of bands) with respect to a reference vector

Response (vector) for similar change events should have a similar angle with respect to a reference vector

$$\theta = cos^{-1}\left(\frac{\vec{\rho}.\vec{u}}{\sqrt{\vec{\rho}^2}\sqrt{\vec{u}^2}}\right)$$ $\vec{u}$: reference vector

Feature/ band selection – most responsive bands (top b) or highest reconstruction error

Clustering spectral angle θ (reference vector and normalized response)

Change Event Separability from Spectral Deviation

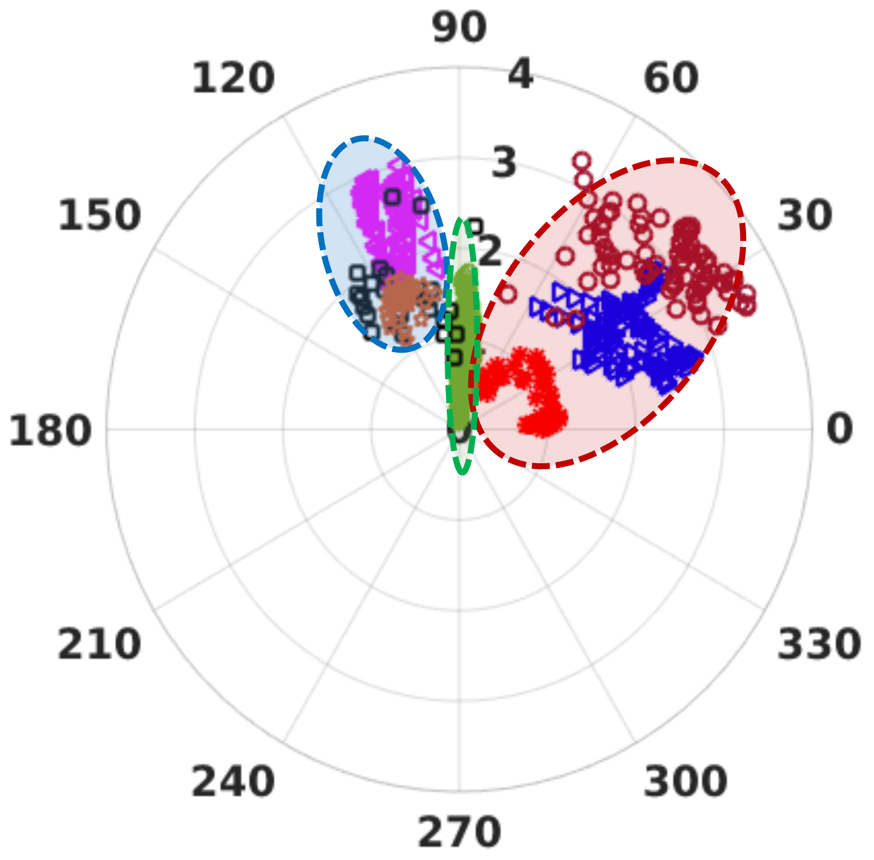

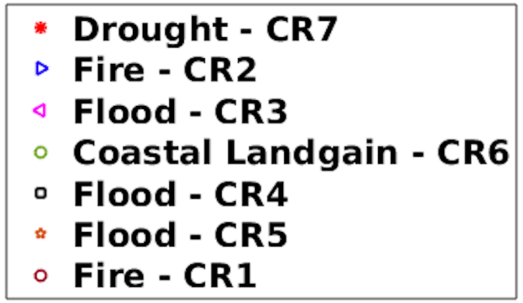

CR1: Wallow Fire (Southwestern United States)
CR2: Horseshoe 2 Fire (Southwestern United States)
CR7: Drought: Southwestern United States
CR3: Flood (Coastal Marsh, Louisiana)
CR4: Flood (Agricultural/ Urban Area, Sava River, Croatia)
CR5: Flood (Agricultural/ Urban Area, Sava River, Bosnia and Herzegovina)
CR6: Land Gain: Atchafalaya Delta Region

Gaussian mixture modeling with varying k(number of clusters)
- Smallest k with lowest sum of error assignment to cluster mean

Graph Connected Components
- Graph Laplacians

Polar coordinate representation of change vector deviations

Conclusion

- Multispectral deviation as change signature
- Detection improves with parameters extracted by Sequential Monte Carlo
- Change events are observed to be separable: jointly consider change event, pre-change class
- Generalized change detection approach

  S. Chakraborty, S. Das, P. R. Christensen, and A. Papandreou-Suppappola, “On the Separability and Explanations of Land Cover Change Events from Multispectral MODIS Time-Series ”
- Future Work: Post change monitoring, time-varying frequency models

References

1. R. S. Lunetta, J. F. Knight, J. Ediriwickrema et al., “Land-cover change detec- tion using multi-temporal MODIS NDVI data,” Remote Sensing of Environment, vol. 105, pp. 142–154, 2006.
2. S. Lhermitte, J. Verbesselt, W. W. Verstraeten, and P. Coppin, “A compari- son of time series similarity measures for classification and change detection of ecosystem dynamics,” Remote Sensing of Environment, vol. 115, pp. 3129–3152, 2011.
3. W. Kleynhans, J. C. Olivier, K. J. Wessels et al. Detecting land cover change using an extended Kalman filter on MODIS NDVI, time-series data,” IEEE Geosci. Remote Sens. Lett., vol. 8, pp. 507–511, 2011.
4. A. Anees, J. Aryal, M. M. OReilly, and T. J. Gale, “A relative density ratio-based framework for detection of land cover changes in MODIS NDVI time series,” IEEE Journal of Selected Topics in Applied Earth Observations and Remote Sensing, vol. 9, no. 8, pp. 3359–3371, 2015.
5. S. Chakraborty, A. Banerjee, S. K. Gupta, P. R. Christensen, and A. Papandreou-Suppappola, “Time-varying modeling of land cover change dy- namics due to forest fires,” IEEE Journal of Selected Topics in Applied Earth Observations and Remote Sensing, vol. 11, no. 6, pp. 1769–1776, 2018.

Questions?